A theory for the core of a leading-edge vortex

By M. G. HALL

Royal Aircraft Establishment, Farnborough, Hampshire

(Received 28 February 1961)

In the flow past a slender delta wing at incidence one can observe a roughly axially symmetric core of spiralling fluid, formed by the rolling-up of the shear layer that separates from a leading edge. The aim in this paper is to predict the flow field within this vortex core, given appropriate conditions at its outside edge.

The basic assumptions are (i) that the flow is continuous and rotational, and (ii) that viscous diffusion is confined to a relatively slender subcore. In addition it is assumed that the flow is axially symmetric and incompressible. Together, these admit outer and inner solutions for the core from the equations of motion. For the outer solution the subcore is ignored, and the flow is taken to be inviscid (but rotational) and conical. The resulting solution consists of simple expressions for the velocity components and pressure. For the inner solution, which applies to the diffusive subcore, the flow is taken to be laminar, and certain approximations are made, some based on the boundary conditions and some analogous to those of boundary-layer theory. The solution obtained in this case is a first approximation, and has been computed.

A sample calculation yields results which are in good qualitative and fair quantitative agreement with experimental measurements.

1. Introduction

A core of spiralling fluid can be observed in the flow past a slender delta wing at incidence. Its position is shown in figure 1, which is a sketch of the over-all flow pattern. Separation of a shear layer takes place from the neighbourhood of each leading edge. The layer curves upward and inboard and eventually rolls up, forming a core in which the velocity and pressure fields are roughly axially symmetric. This over-all pattern is well established experimentally. It appears essentially unchanged through the speed range and for most operating incidences as long as the leading edges are subsonic, and it is found also with slender wings other than deltas. Such a vortex core may have a diameter as large as one-third of the semi-span, and within it have been found velocities so high and pressures so low as to create some speculation and controversy. The aim in this paper is to predict theoretically the velocity and pressure fields within a core, given appropriate conditions at its outside edge, and to explain the core structures that have been observed.

The recent experimental studies by Earnshaw (1961) and Lambourne &

Bryer (1959) have established the structural form taken by the vortex core. Figures 2–5 show results at 70 % chord of measurements by Earnshaw over a delta wing of aspect ratio one and 56 in. centre line, at 14·9° incidence and with a free-stream velocity of 100 ft./sec. Figure 2 is a cross-sectional view showing the formation of the core. The closed contour drawn as a broken line marks the

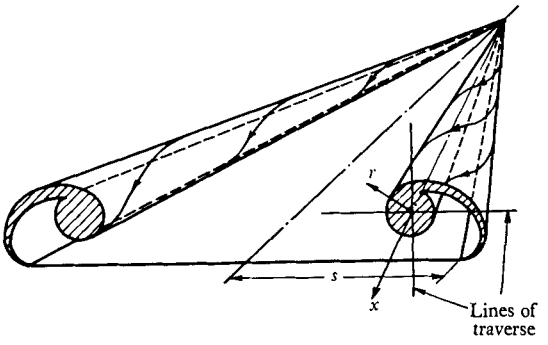

FIGURE 1. Basic pattern for flow over a slender delta wing at incidence.

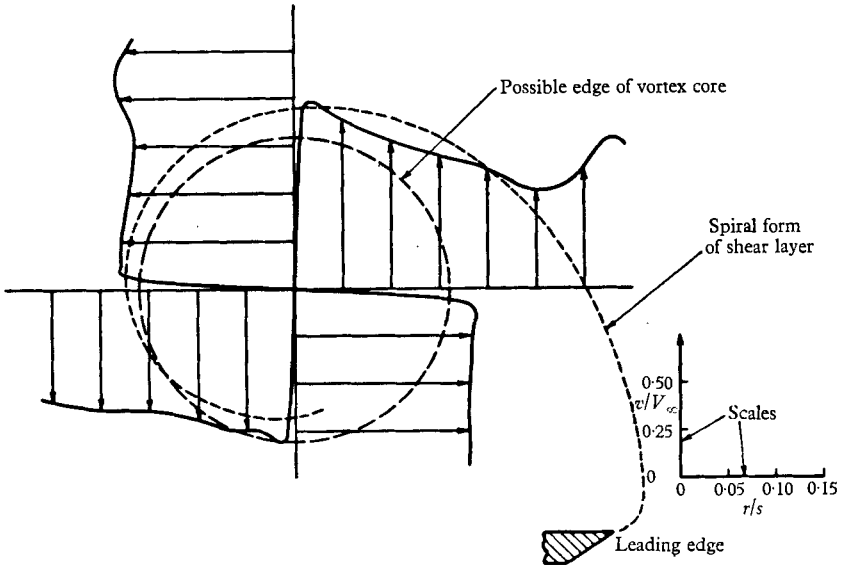

FIGURE 2. Profiles of the circumferential velocity v, derived from Earnshaw's measurements.

outside edge of the core (its size is somewhat arbitrary), the choice being guided only by the criterion of axial symmetry. The ordinate r/s is the ratio of the radial distance r from the axis of the core to the semi-span s (see figure 1). V_∞ is the free-stream velocity. Figures 3–5 show pairs of profiles obtained by traversing through the core in a pair of mutually perpendicular directions (figure 1). Corresponding theoretical profiles are included also: these will be referred to after the theory has been presented. The striking feature here is that there are axial velocities (figure 3) within the core over twice the magnitude of the free

stream velocity and, associated with them, pressure coefficients (figure 5) of less than -6. This stands in sharp contrast to the much smaller perturbations of the free-stream values elsewhere over the wing.

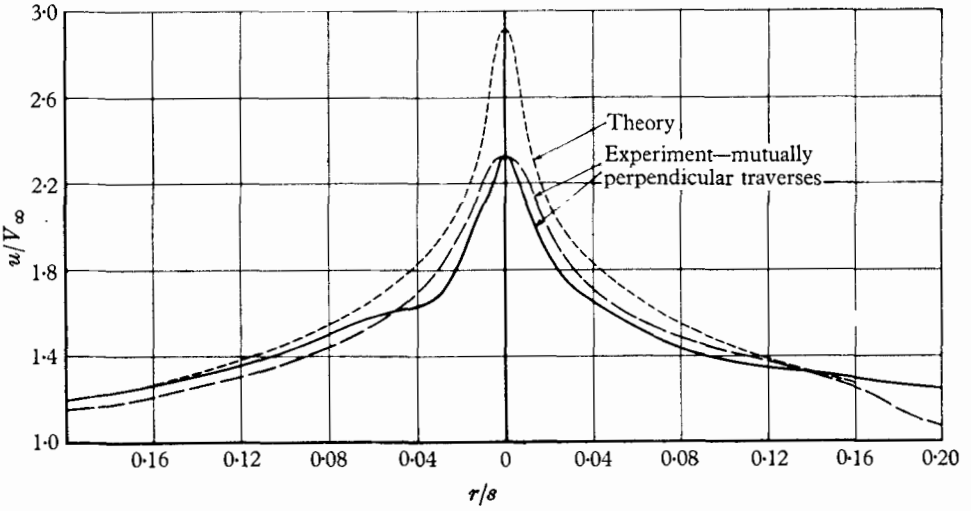

FIGURE 3. Experimental and theoretical profiles of axial velocity u.

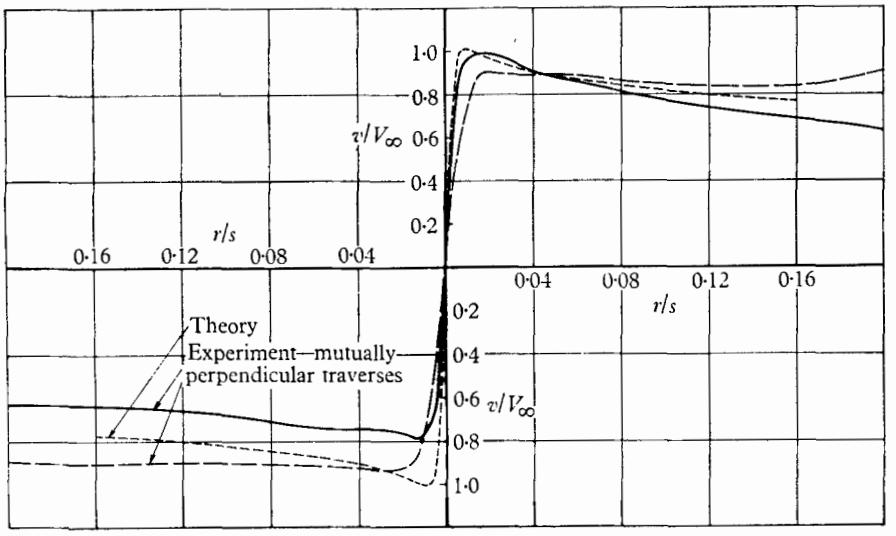

FIGURE 4. Experimental and theoretical profiles of circumferential velocity v.

Certain other features of the observed core structure should be noted, since they suggest the form of a possible simplified model of the core. First, the shear layer from the leading edge diffuses rapidly (figure 2) and is barely distinguishable after less than one convolution of a spiral, before the core is even reached. Secondly, the gradients of total pressure within the core (figure 5) are small except for a very slender region along the axis. It has been found that where the gradients

of total pressure are small the velocity and pressure fields are approximately conical, which is consistent with Jones's wing theory.

A simplified model of the vortex core is adopted here, with two distinctive properties that are suggested by the above. The first property is that the flow is continuous, i.e. it includes no vortex sheet. Thus, the flow must be rotational to allow a convection of vorticity. The second is that diffusion of vorticity (associated with a loss of total pressure) is confined to a relatively slender subcore. In this way the core is divided into a convective outer part and a diffusive subcore. This is justifiable for large Reynolds numbers, and it reduces the problem of solving

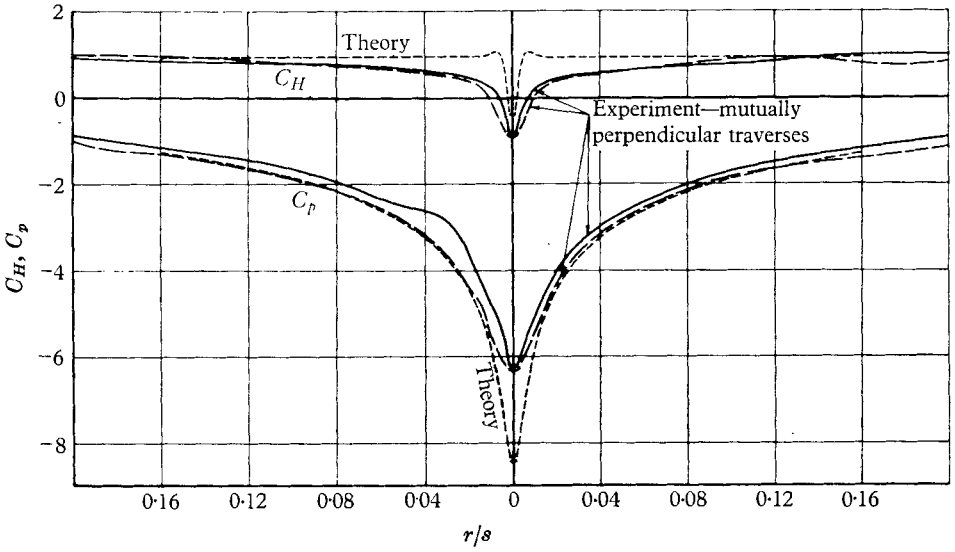

FIGURE 5. Experimental and theoretical profiles of total and static pressure coefficients, $C_H = (p_0 - p_\infty)/\frac{1}{2}\rho V_\infty^2$ and $C_p = (p - p_\infty)/\frac{1}{2}\rho V_\infty^2$ respectively.

the equations of motion for the core to that of obtaining an inviscid outer solution for the convective part—for which the subcore is ignored—and then, using this outer solution to specify boundary conditions, obtaining a viscous inner solution for the subcore. In addition to the distinctive properties, the fluid is taken to be incompressible, and the velocity and pressure fields are taken to be axially symmetric. For the outer solution, these fields are taken to be conical as well, which implies a constant total pressure. Advantage will be taken of the fact that the core is slender to neglect terms of order $(r/x)^2$, where, as shown in figure 1, x is the distance along the axis of the core from the apex of the wing. For the inner solution the flow is taken to be laminar, and the Reynolds number will be supposed to be large enough for approximations analogous to those of boundary-layer theory to be made.

Mangler & Smith (1959) have previously obtained a solution for the vortex core in the course of investigating the flow past the wing as a whole. No specific steps were taken to elucidate the core structure in detail. The flow was treated by slender-wing theory, and only constant values through the core of circumferential and axial velocity were obtained.

In the model of Mangler & Smith, the core consists of a tightly rolled vortex sheet (representing the shear layer) imbedded in a potential flow. This provides an exact representation of the core for the flow past a wing in the limit of infinite Reynolds number, and it is of interest to compare such a model with the present one. Corresponding profiles of the circumferential velocity component are sketched in figure 6. Observe that in the present model the steps due to the vortex sheet have been smoothed out, so that no part of the profile can be that of a potential flow. Because finite Reynolds numbers are admitted here, the profile passes smoothly through the axis no matter what its shape in the outer part of the core. This stricter condition is also satisfied by the profile of the hypothetical

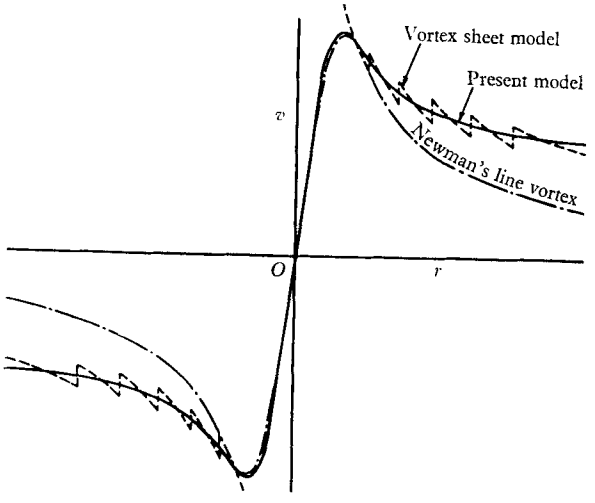

FIGURE 6. Qualitative comparison of different types of profile of the circumferential velocity v.

Rankine vortex, or by a more realistic counterpart, Newman's (1959) theoretical profile for a viscous line vortex of constant strength. A sketch of Newman's profile is included in the figure. If the present profile for a leading-edge vortex were extended far enough from the axis, it would tend to that of a potential flow, as Newman's profile does in the figure. Closer to the axis, the present profile shows (as sketched) a departure from potential flow, as also does Newman's profile. However, the departure in Newman's case is associated solely with a significant increase of viscous diffusion, and leads directly to a 'solid body' rotation, whereas in the present case diffusion is still insignificant and the departure is associated with a convection of vorticity; of course, viscous diffusion eventually does become appreciable here also sufficiently close to the axis. Newman's flow configuration was simple enough for him to obtain a neat approximate solution of the Navier–Stokes equations without having to divide his vortex into outer and inner parts.

2. Outer solution

2.1. *Equations of motion and their solution*

When the velocity and pressure fields are axially symmetric, the Navier–Stokes equations for the steady flow of an incompressible fluid are, in cylindrical coordinates (r, x),

$$\frac{\partial u}{\partial x}+\frac{\partial w}{\partial r}+\frac{w}{r}=0, \tag{1a}$$

$$u\frac{\partial u}{\partial x}+w\frac{\partial u}{\partial r}=-\frac{1}{\rho}\frac{\partial p}{\partial x}+\nu\nabla^2 u, \tag{1b}$$

$$u\frac{\partial v}{\partial x}+w\frac{\partial v}{\partial r}+\frac{vw}{r}=\nu\left(\nabla^2 v-\frac{v}{r^2}\right), \tag{1c}$$

$$u\frac{\partial w}{\partial x}+w\frac{\partial w}{\partial r}-\frac{v^2}{r}=-\frac{1}{\rho}\frac{\partial p}{\partial r}+\nu\left(\nabla^2 w-\frac{w}{r^2}\right), \tag{1d}$$

where

$$\nabla^2\equiv\frac{\partial^2}{\partial r^2}+\frac{1}{r}\frac{\partial}{\partial r}+\frac{\partial^2}{\partial x^2},$$

u and w are the axial and radial velocity components, v is the circumferential velocity component, and p, ρ and ν are the pressure, density and kinematic viscosity, respectively.

The values taken by u, v and w in the outer solution will be denoted by U, V and W respectively. Since the velocity and pressure fields are conical here, U, V, W and p will be functions of the conical parameter $\theta = r/x$ alone. Thus, for the outer solution, where the flow is inviscid (but rotational) and conical, equations (1) reduce to

$$-\theta\frac{d}{d\theta}\left(U-\frac{W}{\theta}\right)+\frac{2W}{\theta}=0, \tag{2a}$$

$$-\left(U-\frac{W}{\theta}\right)\frac{dU}{d\theta}=\frac{1}{\rho}\frac{dp}{d\theta}, \tag{2b}$$

$$-\theta\left(U-\frac{W}{\theta}\right)\frac{dV}{d\theta}+\frac{VW}{\theta}=0, \tag{2c}$$

$$-\theta\left(U-\frac{W}{\theta}\right)\frac{dW}{d\theta}-\frac{V^2}{\theta}=-\frac{1}{\rho}\frac{dp}{d\theta}. \tag{2d}$$

The boundary conditions are taken to be

$$\left.\begin{aligned}&\theta=0, \quad W=0,\\ &\theta=\theta_2, \quad U=U_2, \quad V=V_2, \quad p=p_2,\end{aligned}\right\} \tag{3}$$

where the subscript 2 identifies quantities at the outside edge of the core $\theta = \text{const.} = \theta_2$. The subscript 1 will identify quantities at the outside edge of the subcore. Observe that the solution is here formally extended to the axis, $\theta = 0$, following the stipulation that the viscous subcore is relatively slender. The tacit assumption is that the effects of the subcore on the outer part of the core are negligible. The first condition, that of zero radial flow on the axis, is an

important one. It expresses a continuity condition and implies an absence of sources or sinks. It appears to be the sole condition applicable to the axis of an inviscid rotating flow, for infinite velocities and gradients cannot be ruled out. The ratio V/U, which is a measure of the helix angle of the spiralling streamlines, will appear frequently, and is therefore denoted by the symbol ϕ. The value ϕ_2 may be related to the rate of increase of the strength of the core along its length or, what is equivalent, to the rate at which vorticity is fed in, by taking the circulation $2\pi r_2 V_2$ around the core as a measure of its strength and differentiating: thus

$$\frac{d}{dx}(2\pi r_2 V_2) = 2\pi U_2 \theta_2 \phi_2.$$

The equations (2) are easily integrated. Equations $(2a)$ and $(2c)$ yield

$$\left(\frac{V}{V_2}\right)^2 = \frac{U - W/\theta}{U_2 - W_2/\theta_2}. \tag{4}$$

Equation (4), together with $(2a)$ and $(2b)$, enables V and p to be eliminated from equation $(2d)$, which becomes

$$(1+\theta^2)\frac{dW}{d\theta} + \frac{W}{\theta} = -\frac{V_2^2}{U_2 - W_2/\theta_2}. \tag{5}$$

Therefore, since the term $\theta^2 = (r/x)^2$ in the bracket may be neglected for a slender core,† the solution for W is

$$\left.\begin{aligned} W/W_2 &= \theta/\theta_2, \\ W_2 &= -\tfrac{1}{2}(\theta_2 U_2)\{\sqrt{(1+2\phi_2^2)} - 1\} < 0. \end{aligned}\right\} \tag{6}$$

Note that $\sqrt{(1+2\phi_2^2)}$ is positive; the possible ambiguity of sign in the expression for W_2 has been removed by applying the condition $W/U < \theta$, which follows from Kelvin's circulation theorem. The substitution of (6) in equation $(2a)$ leads to the result

$$\frac{U}{U_2} = 1 - \{\sqrt{(1+2\phi_2^2)} - 1\}\log\left(\frac{\theta}{\theta_2}\right), \tag{7}$$

and the substitution of (6) and (7) in (4) yields

$$\left(\frac{V}{V_2}\right)^2 = 1 - \left[\frac{\sqrt{(1+2\phi_2^2)} - 1}{\phi_2}\right]^2 \log\left(\frac{\theta}{\theta_2}\right). \tag{8}$$

Finally, the neglect of the term θ^2 in equation (5) implies that $(2d)$ can be reduced to

$$\frac{1}{\rho}\frac{dp}{d\theta} = \frac{V^2}{\theta}; \tag{9}$$

and the expression for V^2 given by equation (8) enables this to be integrated, with the result

$$\frac{p - p_2}{\rho V_2^2} = \log\left(\frac{\theta}{\theta_2}\right) - \frac{1}{2}\left[\frac{\sqrt{(1+2\phi_2^2)} - 1}{\phi_2}\right]^2 \log^2\left(\frac{\theta}{\theta_2}\right). \tag{10}$$

† Equation (5) can be solved without neglecting θ^2, but the expressions for the other velocity components then become unduly complicated for this particular problem.

2.2. *Discussion of the outer solution*

Equations (6), (7), (8) and (10) constitute a solution for the flow in the convective outer part of the core. Equations (6) show that the radial flow is always small and always directed inwards toward the axis, and that it decreases linearly in magnitude with decreasing distance from the axis. Also, the larger the ratio ϕ_2,

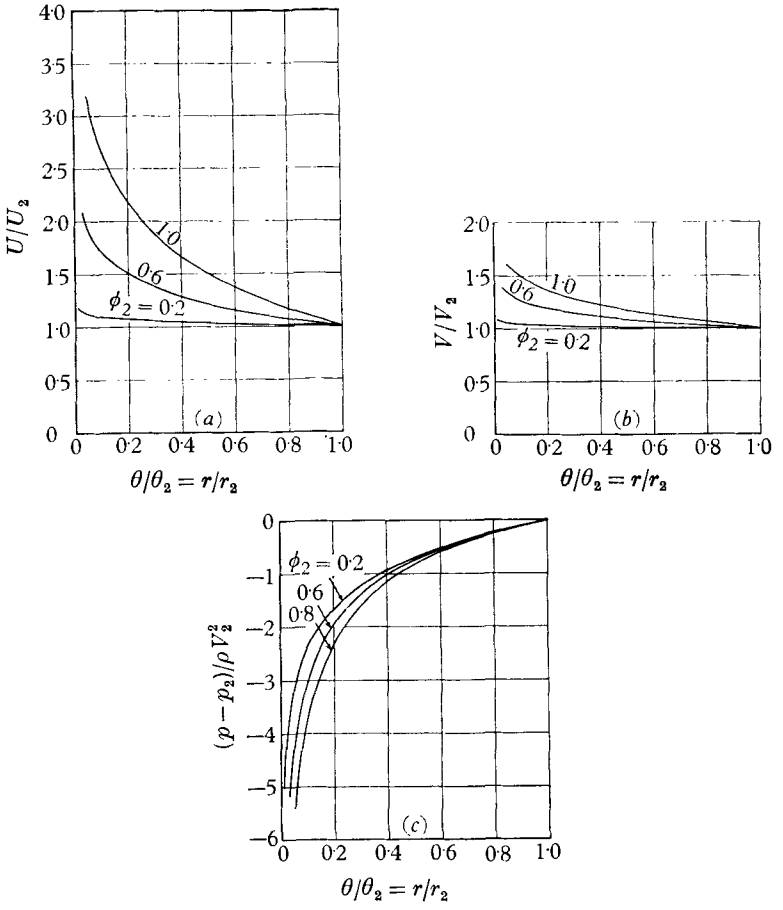

FIGURE 7. Profiles from the outer solution, showing the effect of varying ϕ_2, for (*a*) the axial velocity U, (*b*) the circumferential velocity V, and (*c*) the static pressure p.

the larger is the radial in-flow. Some representative profiles of the axial and circumferential velocity components U and V and of the pressure p have been calculated from equations (7), (8) and (10), respectively, and are shown in figure 7. The abscissae on the figures denote the non-dimensional distance from the axis of symmetry. Each figure is concerned with one of the velocity components or with the pressure, and the different curves in the figure correspond to different values of ϕ_2.

The figures show that U/U_2, V/V_2 and the pressure drop $(p_2-p)/\rho V_2^2$ all decrease with increasing distance from the axis, and all increase with increasing ϕ_2. It may be observed that the increase in axial velocity U and the drop in pressure

within the core may be very considerable. Such a pressure drop is to be expected in a spiralling flow, but the considerable increase in axial velocity is perhaps surprising. This increase is, however, a natural consequence of the original assumptions of conical field, etc., for the structure of the core. The phenomenon may be easier to understand if it is noted that according to the theory the pressure gradient in the direction of the spiralling path of a fluid element is negative and sustained, though not in general large: the core is such that it entrains fluid and retains it in a pressure field, which subjects each element to a continuous accelerating force. Alternatively, it can be shown that the vortex lines in the outer solution nearly coincide with the spiralling streamlines, so that there exists a circumferential component of vorticity for which the induced flow is axial. Since the distribution of this vorticity is symmetrical about the axis of the core, there will be, in effect, a focusing or concentrating action which yields a high resultant velocity along the axis.

The outer solution is clearly singular on the axis of symmetry, but even as the axis is approached the solution becomes invalid. Towards the axis, the gradients of vorticity become increasingly large, so that it is to be expected that viscous diffusion will become appreciable. In addition, according to equation (10) the pressure p becomes negative for sufficiently small θ/θ_2. It is supposed here, however, that before this occurs the diffusion effects have invalidated the solution. An *a posteriori* check of the viscous diffusion effects implied by the outer solution is therefore worth while.

The procedure is to feed back the above (inviscid) solutions for U, V and W into the full Navier–Stokes equations (1), and to compare the magnitudes of the terms representing inertia and viscous forces. It can be shown, if this is done, that the outer solution implies negligible viscous forces in the axial direction. But circumferential viscous forces are implied: the ratio of inertia to viscous terms, if we assume that ϕ_2 is not large compared with unity, is found to be

$$O\left(\frac{\phi^2 U x\theta^2}{\nu}\right) = O\left(\frac{\phi_2^2 U_2 x\theta^2}{\nu}\right).$$

The product

$$\phi_2^2 R_2 \equiv \frac{\phi_2^2 U_2 x}{\nu}$$

is of special significance. It is clear that in a region of dimensions $\theta = O(\phi_2^{-1} R_2^{-\frac{1}{2}})$ diffusion effects must become appreciable, and the outer solution must become unrealistic. Thus it can be deduced from the outer solution that a diffusive subcore exists and, moreover, that circumferential viscous forces play the dominant role in its generation. Note that this subcore can be made as slender as desired by taking R_2 sufficiently large. The limit (with ϕ_2 bounded) $R_2 \to \infty$ therefore constitutes the formal condition for the present model of the vortex core to be self-consistent, because only in this limit will an inviscid outer flow which is conical be compatible with an inner diffusive subcore which cannot be conical. Note finally that as $R_2 \to \infty$ then, for the edge of the subcore, $\theta_1/\theta_2 \to 0$, and, from equations (7) and (8),

$$\frac{V_1^2}{U_1^2} \equiv \phi_1^2 \to 0.$$

3. Inner solution†

3.1. *Approximation of the equations of motion*

Equations (1) apply to the diffusive subcore, but they are intractable as they stand. In this subsection, approximations will be made to simplify the equations. What is wanted is an approximate solution valid for large but finite Reynolds numbers. The first step would be to make the usual boundary-layer assumptions (that the Reynolds number tends to infinity, and so on), and to seek an inner solution which satisfies the proper conditions on the axis of symmetry and tends asymptotically to the outer solution with increasing distance from the axis. If no more than this is done, however, it is found that the equations of motion are still intractable, mainly because large variations of the axial velocity are not excluded. Fortunately, the boundary-layer assumptions can be coupled with other assumptions based on the boundary conditions. The symbols u, v, w will be retained for the velocity components within the subcore. On the axis of symmetry, $r = 0$, a diffusive fluid satisfies the conditions

$$\frac{\partial u}{\partial r} = v = w = 0.$$

At the edge, $r = r_1$, of the subcore, we have, in the limit as viscous diffusion becomes negligible,

$$u = U_1, \quad v = V_1 \quad \text{and} \quad p = p_1.$$

The assumptions suggested by the above boundary conditions are, first, that

$$u = \text{const.} + O(\epsilon u), \tag{11a}$$

where ϵ is small; secondly, since the outer solution suggests (§ 2.2) that axial viscous forces will not be significant in the outer part $r > \delta$, say, of the subcore,

$$\left.\begin{aligned} \left(\frac{\partial u}{\partial r}\right)_{r \geqslant \delta} &= O\left(\frac{\partial U}{\partial r}\right), \\ \left(\frac{\partial u}{\partial r}\right)_{r < \delta} &= O\left[\left(\frac{\partial U}{\partial r}\right)_{r=\delta}\right]; \end{aligned}\right\} \tag{11b}$$

and, thirdly,

$$w = O(W) = O(W_1 r/r_1). \tag{11c}$$

The first of these, (11a), will be justified eventually: it is not introduced merely to simplify the equations of motion. An expression for ϵ,

$$\epsilon = \phi_1^2 \log(\theta_1 R_1^{\frac{1}{2}}), \tag{12}$$

can be deduced, by establishing from equation (1b) that $\delta = O(xR_1^{-\frac{1}{2}})$ and integrating $\partial u/\partial r$. But it can be shown from the outer solution that $\theta_1 R_1^{\frac{1}{2}}$ is large for large Reynolds numbers. If ϵ is to be small, therefore, a limit will have to be placed on the magnitude of $\theta_1 R_1^{\frac{1}{2}}$.

The assumptions similar to those made in boundary-layer theory are that (i) the Reynolds number is large or, formally, $R_2 \to \infty$, and (ii) the circum-

† A more detailed account has been given (1960) by the author.

ferential viscous forces, which have the dominant role in generating the subcore, must be as important as the circumferential inertia forces (within the subcore) and must be negligible at the edge.

These two sets of assumptions—from the boundary conditions and from boundary-layer theory—enable the orders of magnitude of the terms in equations (1) to be specified in such a way that solution becomes practicable. Now, as pointed out in the previous section, the condition $R_2 \to \infty$ implies that $\theta_1/\theta_2 \to 0$ and that $\phi_1^2 \to 0$. The basis of the present approximation to the equations of motion will be to make use of the smallness of ϕ_1^2 and ϵ to simplify the equations. ϕ_1^2 will be treated as a small parameter; unlike θ_1/θ_2, it remains a meaningful parameter for finite Reynolds numbers. It can be deduced from the outer solution that, for $\phi_1^2 \to 0$,

$$\phi_1^2 = -\frac{1}{\log \theta_1} = -\frac{2W_2}{\theta_2 U_1} = -\frac{2W_1}{\theta_1 U_1}, \tag{13}$$

so that ϕ_1^2 is a measure not only of the helix angle of the spiralling streamlines at the edge of the subcore but also of the rate of convergence of the streamlines.

On neglect of the terms in equations (1) that are smaller by a factor of either ϕ_1^2 or ϵ, the equations reduce to

$$\frac{\partial u}{\partial x} + \frac{\partial w}{\partial r} + \frac{w}{r} = 0, \tag{14a}$$

$$U_1 \frac{\partial u}{\partial x} = -\frac{1}{\rho}\frac{\partial p}{\partial x} + \nu\left(\frac{\partial^2 u}{\partial r^2} + \frac{1}{r}\frac{\partial u}{\partial r}\right), \tag{14b}$$

$$U_1 \frac{\partial v}{\partial x} + w\frac{\partial v}{\partial r} + \frac{vw}{r} = \nu\left(\frac{\partial^2 v}{\partial r^2} + \frac{1}{r}\frac{\partial v}{\partial r} - \frac{v}{r^2}\right), \tag{14c}$$

$$\frac{v^2}{r} = \frac{1}{\rho}\frac{\partial p}{\partial r}. \tag{14d}$$

As the equations stand, they are still intractable, but clearly if some approximation to w could be substituted in (14*c*), so that the equation yielded a satisfactory first approximation to v, completion of the solution would be straightforward. Now, for $r \ll r_1$, the terms in (14*c*) containing w become negligible anyway, so that any chosen w need be an adequate approximation to the correct w for larger r only. The obvious choice, therefore, is the formula given by equations (6) respective to the outer solution, namely

$$w = \frac{W_2}{\theta_2}\frac{r}{x}.$$

Thus w is assigned its correct magnitude and gradient at $r = r_1$, and its correct magnitude at $r = 0$. Substitution in equation (14*c*) yields

$$U_1 \frac{\partial v}{\partial x} + \frac{W_2}{\theta_2}\frac{r}{x}\frac{\partial v}{\partial r} + \frac{W_2}{\theta_2}\frac{v}{x} = \nu\left(\frac{\partial^2 v}{\partial r^2} + \frac{1}{r}\frac{\partial v}{\partial r} - \frac{v}{r^2}\right). \tag{15}$$

The equations (15), (14*d*), (14*b*) and (14*a*) can be solved successively, to yield first approximations to v, p, u and w, respectively. This would in fact be the first step in a process of solution by iteration. In this process the adoption of the

formula given by the outer solution for w would constitute the 'zeroth' approximation. However, only the first approximations will be sought here, and whether the process of iteration is justified will be put aside.

3.2. *Transformation of the equations and the form of the solution*

The equations for the subcore are still not easy to solve, because they contain partial derivatives. This would be remedied if, by transformation of the variables, similar solutions could be found. A new independent variable

$$\zeta = \left[\frac{U_1(x)\,x}{\nu}\right]^{\frac{1}{2}} \frac{r}{x} \tag{16}$$

is therefore introduced to replace r as the measure of the radial distance from the axis. For the region within which viscous diffusion must, according to the *a posteriori* check, become appreciable, it can be shown that $\zeta^2 = O(1/\phi_1^2)$; and, for the edge of the subcore, $\zeta_1^2 \gg 1/\phi_1^2$. Similar solutions of the form

$$u = U_1(x) f(\zeta), \quad v = V_1(x)\, g(\zeta), \quad \zeta_1 = \text{const.} \tag{17}$$

will be sought, where $df/d\zeta = g = 0$ at $\zeta = 0$ and $f = g = 1$ at $\zeta = \zeta_1$. The value of ζ_1 may be arbitrarily chosen, provided it is large enough to satisfy the condition $\zeta_1^2 \gg 1/\phi_1^2$ and not so large that the assumption (11*a*) is invalidated.

Equations (15), (14*d*), (14*b*) and (14*a*) are now transformed by substitution of the new variables f, g and ζ. After some labour, in which the outer solution is used, terms that are smaller by the factors ϕ_1^2 and ϵ are again neglected, and the result is

$$\frac{d^2g}{d\zeta^2} + \left(\frac{\zeta}{2} + \frac{1}{\zeta}\right)\frac{dg}{d\zeta} + \left(\frac{\phi_1^2}{4} - \frac{1}{\zeta^2}\right) g = 0, \tag{18}$$

$$\frac{1}{\rho}\frac{\partial p}{\partial \zeta} = V_1^2 \frac{g^2}{\zeta}, \tag{19}$$

$$\frac{d^2f}{d\zeta^2} + \left(\frac{\zeta}{2} + \frac{1}{\zeta}\right)\frac{df}{d\zeta} = -\frac{\phi_1^2}{2} g^2 + \frac{\phi_1^4}{2}\int_{\zeta_1}^{\zeta} \frac{g^2}{\zeta}\, d\zeta, \tag{20}$$

$$\left(\frac{x}{\nu U_1}\right)^{\frac{1}{2}} \frac{\partial}{\partial \zeta}(\zeta w) = -\frac{\phi_1^2}{2}\zeta + \frac{\zeta^2}{2}\frac{df}{d\zeta}. \tag{21}$$

It is clear from equations (18) to (21) that the form of solution specified by equations (17) is compatible with the equations of motion. Therefore, since the boundary conditions are already satisfied, the similar solutions (17) exist, and the calculations of the solutions can proceed.

3.3. *Solutions of the transformed equations*

Once a solution for g is obtained from equation (18), solutions for p, f and w are readily derived. The solution of equation (18) is

$$\begin{aligned} g = kG(\phi_1^2, \zeta) &= k\zeta \exp\left(-\tfrac{1}{4}\zeta^2\right) {}_1F_1\left(\tfrac{3}{2} - \tfrac{1}{4}\phi_1^2, 2, \tfrac{1}{4}\zeta^2\right) \\ &= k\zeta \exp\left(-\tfrac{1}{4}\zeta^2\right)\left[1 + \frac{\frac{3}{2} - \frac{1}{4}\phi_1^2}{2}\,\tfrac{1}{4}\zeta^2 + \frac{\left(\frac{3}{2} - \frac{1}{4}\phi_1^2\right)\left(\frac{5}{2} - \frac{1}{4}\phi_1^2\right)}{2! \times 2 \times 3}\left(\tfrac{1}{4}\zeta^2\right)^2 + \ldots\right], \end{aligned} \tag{22}$$

where k is a constant fixed by the boundary condition $g = 1$ at $\zeta = \zeta_1$, and ${}_1F_1$ is a confluent hypergeometric function (see, for example, Jeffreys & Jeffreys 1956, ch. 23).

By substituting $kG(\phi_1^2, \zeta)$ for g, equations (19) and (20) can be integrated to yield p and f respectively, and substitution for $df/d\zeta$ in (21) then enables w to be calculated. The results may be expressed in the forms

$$f = 1 + k^2\phi_1^2[(F_1 - F) + \phi_1^2(\alpha_1 - \alpha)P_1], \tag{23}$$

$$\frac{w}{W_2} = \frac{\theta}{\theta_2}[\tfrac{1}{2} + k^2(H + \phi_1^2\beta P_1)], \tag{24}$$

$$\frac{p}{\rho U_1^2} = \frac{p_1}{\rho U_1^2} - k^2\phi_1^2(P_1 - P), \tag{25}$$

where F, H and P are functions of ϕ_1^2 and ζ, given by

$$F = \frac{1}{2}\int_0^\zeta \left\{\frac{1}{\zeta \exp(\frac{1}{4}\zeta^2)}\int_0^\zeta \zeta \exp(\tfrac{1}{4}\zeta^2)\left(G^2 - \phi_1^2\int_0^\zeta \frac{G^2}{\zeta}d\zeta\right)d\zeta\right\}d\zeta,$$

$$H = \frac{1}{2\zeta^2}\int_0^\zeta \left\{\frac{\zeta}{\exp(\frac{1}{4}\zeta^2)}\int_0^\zeta \zeta \exp(\tfrac{1}{4}\zeta^2)\left(G^2 - \phi_1^2\int_0^\zeta \frac{G^2}{\zeta}d\zeta\right)d\zeta\right\}d\zeta,$$

$$P = \int_0^\zeta \frac{G^2}{\zeta}d\zeta,$$

and α and β are functions of ζ only, given by

$$\alpha = \int_0^\zeta \frac{\exp(\frac{1}{4}\zeta^2) - 1}{\zeta \exp(\frac{1}{4}\zeta^2)}d\zeta$$

$$\beta = \frac{1}{\zeta^2}\int_0^\zeta \frac{\zeta[\exp(\frac{1}{4}\zeta^2) - 1]}{\exp(\frac{1}{4}\zeta^2)}d\zeta.$$

To the above may be added an expression for the total pressure p_0, derived from equations (22) to (25) and (17):

$$p_0 = p_{01}(=p_{02}) - \tfrac{1}{2}\rho V_1^2(1 - k^2G^2) - k^2\phi_1^2\rho U_1^2[(P_1 - P) - (F_1 - F) - \phi_1^2(\alpha_1 - \alpha)P_1]. \tag{26}$$

The functions F, G, H and P have been computed for ϕ_1^2 ranging from 0 to 0·6 in increments of 0·1, and the numerical results have been tabulated by the author (1960), together with numerical values of α and β. Curves of the function $G\ (= v/(kV_1))$ are plotted in figure 8. For large ζ, the asymptotic form of the confluent hypergeometric function gives

$$G \doteqdot \frac{2}{(\frac{1}{2} - \frac{1}{4}\phi_1^2)!}\left(\frac{\zeta^2}{4}\right)^{-\frac{1}{4}\phi_1^2}.$$

As might be expected, this is the same as would be obtained from equation (18) if the viscous terms therein were neglected.

Comparison of the solution for G with its asymptotic form indicates how viscous diffusion effects vary within the subcore. Included in figure 8 are the asymptotic curves for the cases $\phi_1^2 = 0$ and $\phi_1^2 = 0{\cdot}6$. It can be seen from these that the effects decrease rapidly as ζ increases, up to about $\zeta = 6$, and that by $\zeta = 10$ they are small. A close examination shows also that the decrease is more marked for

$\phi_1^2 = 0{\cdot}6$ than for $\phi_1^2 = 0$. Thus, the comparison shows the results to be consistent with the condition $\zeta_1^2 \gg 1/\phi_1^2$: the magnitude of ζ at the edge of the subcore must indeed be large for diffusion effects to be vanishingly small, and the smaller the magnitude of ϕ_1^2 the larger must ζ_1 be. But the comparison shows, in addition, that it will be sufficient for a first approximation to take ζ_1 equal to, say, 8 or 10, independently of ϕ_1^2. For although a smaller ϕ_1^2 will imply that diffusion effects will persist to a larger ζ, those effects will be small enough to be neglected anyway for ζ beyond 8 or 10.

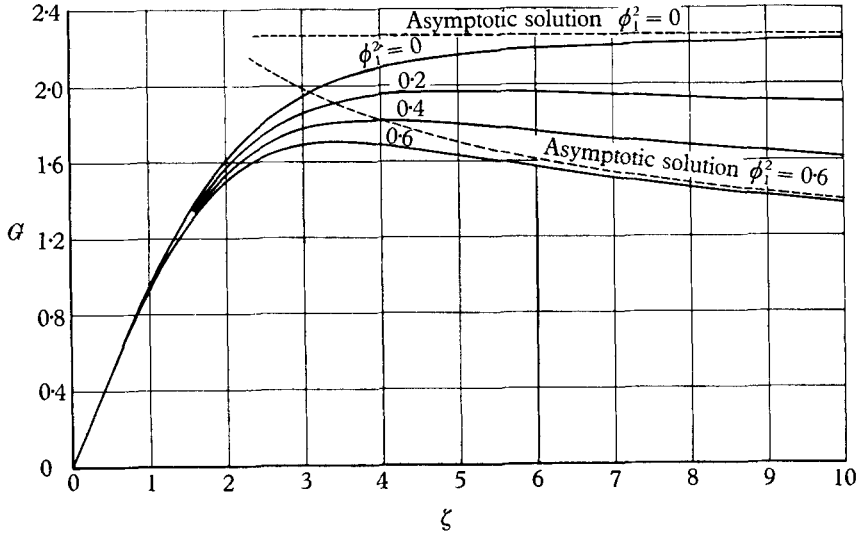

FIGURE 8. Curves of the function G from the inner solution, together with asymptotic solutions, for different values of ϕ_1^2.

Equations (22) to (26), together with (17), constitute an approximate inner solution, and describe the structure of the diffusive subcore. On the axis the circumferential and radial velocity components, v and w, are zero, and so also are the radial gradients of the axial velocity u, the static pressure p, and the total pressure p_0, with u taking a maximum value and p and p_0 minimum values there. The circumferential velocity is a maximum at a distance from the axis which decreases with both increasing ϕ_1^2 and increasing R_2. The radial velocity, which describes an inward flow, grows with increasing distance from the axis, from half the magnitude given by the outer solution. The circumferential and axial components, and the pressures, have magnitudes at the edge of the subcore equal to those given by the outer solution.

From the inner solution the effects of variations of Reynolds number can be worked out, and a brief illustration of this is given in the following section.

3.4. *Reynolds number effects*

Given a vortex core for which θ_2, U_2/V_∞, V_2/V_∞ and $C_{p2} = (p_2 - p_\infty)/\frac{1}{2}\rho V_\infty^2$ are specified, what are the effects of variations of the Reynolds number $R = V_\infty x/\nu$ on the core structure? Evidently the effects must be confined to the subcore.

As suggested in the previous subsection, ζ_1 is taken to be constant, independent of ϕ_1^2 and, consequently, independent of R. Such a constant ζ_1 is in fact a measure of the size of a subcore, for, as can be seen in figure 8, the range of ζ over which viscous diffusion effects become small is roughly the same for different solutions of the subcore.

From equations (16) and (7), we get

$$\zeta_1 = R^{\frac{1}{2}}\left(\frac{U_2}{V_\infty}\right)^{\frac{1}{2}}\theta_1\left(\frac{U_1}{U_2}\right)^{\frac{1}{2}} = R^{\frac{1}{2}}\left(\frac{U_2}{V_\infty}\right)\theta_1\left[1-\{\sqrt{(1+2\phi_2^2)}-1\}\log\left(\frac{\theta_1}{\theta_2}\right)\right]^{\frac{1}{2}} = \text{const.} \tag{27}$$

It follows that $d\theta_1/dR < 0$, or that θ_1 decreases as R increases. θ_1 is a direct measure of the slenderness of the subcore: the larger the Reynolds number, the slenderer is the subcore.

A number of trends can be deduced. Suppose the Reynolds number is increased from R to R', so that $\theta_1' < \theta_1$. From equations (7), (8) and (10), respectively, $U_1' > U_1$, $V_1' > V_1$, and $p_1' < p_1$. Since $U_1' > U_1$, equation (13) yields $\phi_1'^2 < \phi_1^2$. From equations (17), (13) and (23), it appears that

$$u'_{\max} - u_{\max} = \frac{2W_2}{\theta_2}[k^2(F_1+\alpha_1\phi_1^2P_1)+\phi_1^2-k'^2(F_1'+\alpha_1\phi_1'^2P_1')-\phi_1'^2],$$

and from equations (25) and (26), respectively, again with use of (13),

$$p'_{\min} - p_{\min} = p_1' - p_1 + \frac{4\rho W_2^2}{\theta_2^2}\left[\frac{k^2P_1}{\phi_1^2}-\frac{k'^2P_1'}{\phi_1'^2}\right],$$

and $$p'_{0\min} - p_{0\min} = \tfrac{1}{2}\rho V_1^2 - \tfrac{1}{2}\rho V_1'^2 + \frac{4\rho W_2^2}{\phi_2^2}\left[\frac{k^2}{\phi_1^2}(P_1-F_1-\alpha_1\phi_1^2P_1)-\frac{k'^2}{\phi_1'^2}(P_1'-F_1'-\alpha_1\phi_1'^2P_1')\right].$$

Now it can be checked from the tables that, for $\zeta_1 = 8$ or 10, each of the expressions in square brackets in the above three equations is negative. Furthermore, $p_1' < p_1$ and $V_1' > V_1$. Therefore the three equations yield $u'_{\max} > u_{\max}$, $p'_{\min} < p_{\min}$, and $p'_{0\min} < p_{0\min}$. Thus an increase of the Reynolds number yields, on the axis, an increase of the velocity and a lowering of both the static and total pressures. Alternatively, for any particular vortex core, the Reynolds number $R = V_\infty x/\nu$ grows with the distance x from the apex. Along the axis, therefore, the velocity increases, and the static and total pressures drop, with increasing distance from the apex.

4. Comparison with experimental results

The above theory has been employed to calculate the velocity and pressure fields within a particular vortex core. For the boundary conditions at the outside edge of the core, numerical values based on Earnshaw's measurements (1961) were used, so that the theoretical results are directly comparable with the experimental profiles of figures 3–5. The numerical results for u/V_∞, v/V_∞ (u and v now are taken to refer also to the outer solution), C_p, and $C_H = (p_0-p_\infty)/\frac{1}{2}\rho V_\infty^2$ have been superimposed on the corresponding experimental results in figures 3–5.

The joining of the inner and outer solutions for u/V_∞, v/V_∞ and w/W_2 is shown in figure 10, but this will be discussed in the final section rather than here.

In addition, the variation with the Reynolds number $R = V_\infty x/\nu$ of $U_{\max}/V_\infty$ in subcores corresponding to the particular outer solution considered here has been calculated for R ranging from $10^{5\cdot5}$ to 10^8. Values of R below $10^{5\cdot5}$ were excluded because, with the present outer solution, errors in the inner solution are then likely to be appreciable. For example, in the experiment $R = 2{\cdot}22 \times 10^6$,

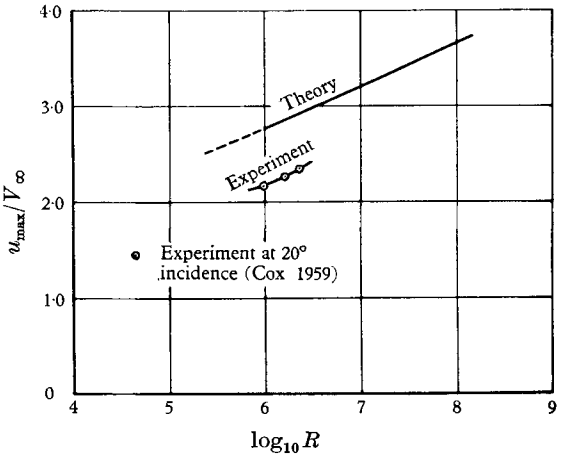

FIGURE 9. Variation with the Reynolds number R of the velocity along the axis of the vortex core of § 4.

and this gives $\phi_1^2 \sim 0{\cdot}2$ and $\epsilon \sim 0{\cdot}4$, whereas the theory requires $\phi_1^2 \ll 1$ and $\epsilon \ll 1$. For smaller R, ϕ_1^2 and ϵ are still larger. It is thus perhaps questionable whether this comparison is a fair test of the theoretical inner solution. The resulting curve of $u_{\max}/V_\infty$ is plotted in figure 9, together with the few available experimental results, and it can be seen that theory and experiment give similar upward trends of $u_{\max}/V_\infty$ with increasing Reynolds number.

Compare now the theoretical and experimental profiles of figures 3–5. The outer solution is seen to give results which agree fairly well with the experimental results. The static pressure profiles, outside the subcore, are in markedly good agreement. That there are some discrepancies may be attributed to the theoretical assumption that the flow field is inviscid, exactly axially symmetric, and exactly conical. On the other hand, the inner solution gives results which differ appreciably from the experimental results: the predictions are only qualitatively correct. The theoretical velocity and pressure gradients in the subcore are too large, and the peaks are too pronounced. The theoretical subcore is too slender. Now, it does not seem likely that instrument errors, or too large a value of ϕ_1^2 or ϵ, can account for the discrepancies. So, while the viscous diffusion outside the subcore and effects of the flow near the apex should not be overlooked, it is natural to question the assumption of laminar flow in the subcore. Measurements by Lambourne & Bryer (1959) in a similar leading-edge vortex have suggested that the flow in the core is turbulent. The poor agreement here also suggests this. If this is so, the laminar theory might still be applied, but only

in a limited way: theoretical and experimental results might be matched by the introduction of an eddy viscosity, for example as Newman (1959) has done. From experience with wakes, the introduction of an eddy viscosity into the theoretical results for laminar flow would give increased diffusion, or a smaller effective Reynolds number, and this would improve the agreement.

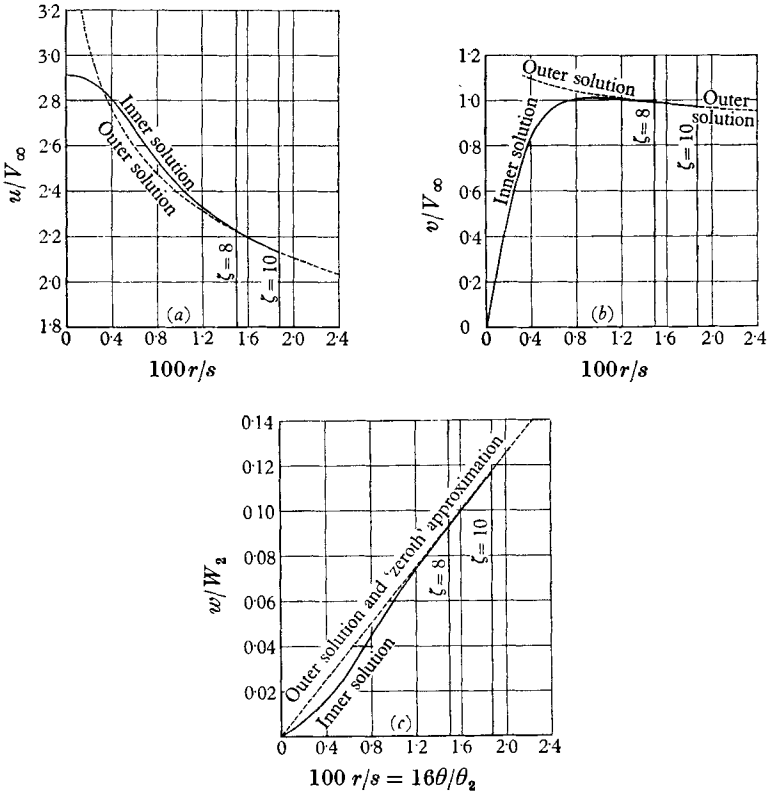

FIGURE 10. Joining of the inner and outer solutions (§4) for (*a*) the axial velocity u, (*b*) the circumferential velocity v, and (*c*) the radial velocity w.

5. Discussion

First, the present work will be briefly summarized. Then, the joining of the inner and outer solutions, and the validity of the theory will be discussed. Finally, some extensions of the work will be considered.

The theoretical results obtained stem from the type of vortex core model originally chosen. The essential features of the model were (i) that the flow is continuous and rotational, and (ii) that viscous diffusion is confined to a relatively slender subcore. Allied with the assumption that the flow is axially symmetric and incompressible, these admitted outer and inner solutions for the core. For the outer solution the subcore was ignored and the flow was taken to be inviscid and conical. The results (§2.1) were in simple logarithmic form. For the inner solution, which applied to the subcore, the flow was taken to be laminar, and approximations, some based on the boundary conditions and some analogous to

those of boundary-layer theory, were made. The results of § 3.3, in this case first approximations, appeared as similar solutions. Given the axial and circumferential velocities, the pressure, and the Reynolds number at the outside edge of the core, the velocity and pressure fields within the core can be calculated. The comparison with experimental results (§ 4) showed fair agreement, except in the details of the subcore, and this does not necessarily imply a fault in the model chosen, because it seems likely that the flow in the subcore of the experiment was significantly turbulent. Over-all qualitative agreement was good.

Figure 10 shows the joining of the profiles of the axial (u), circumferential (v), and radial (w) components of velocity, respectively, for the particular vortex core of § 4. For u and v, the magnitudes given by the inner and outer solutions at $\zeta_1 = 8$ were equated. Each join is seen to be smooth: the gradient is so nearly continuous that the extension of the inner solution to $\zeta_1 = 10$ virtually coincides with the outer solution. ζ_1 could equally well have been taken to be 10, say, but could not have been taken much larger without violating the condition ϵ $(= \phi_1^2 \log \zeta_1) \ll 1$. For w, the only boundary condition satisfied was $w = 0$ at $\zeta = 0$, and yet the inner and outer solutions very nearly coincide at ζ equal to 8 or 10. Had the Reynolds number been larger, even smoother joins could have been obtained.

The smoothness of the joins justifies two assumptions that were introduced tentatively. The first is the approximation made for w in equation (14c). The second is the vital simplifying assumption (§ 3.1) that the variations of axial velocity in the subcore are small, or $\epsilon \ll 1$: since the join *is* smooth, it can be said that at the edge of *some* region for which $\epsilon \ll 1$ does hold, viscous diffusion is indeed negligible, and thus there is a sound physical basis for the assumption.

The above points are related to the internal consistency of the theory. For example, it can be shown from equation (23) that f $(= u/U_1) = 1 + O(\phi_1^2 \log \zeta_1)$, as is required by (11$a$) and (12). Again, it can be shown from the outer solution that as $\theta \to 0$ equations (2) can be reduced to the equations obtained by omitting the viscous terms in (14). Therefore, with increasing distance from the axis, a solution of (14) must tend to one given by (2)—until ϵ and the errors in equations (14) become appreciable and the solutions diverge. For sufficiently large Reynolds numbers there is an intermediate region, where diffusion is negligible and before the solutions diverge, in which a join can be made. This join specifies an approximate solution. The exploitation of the smallness of the variations of the axial velocity in the subcore thus enables an approximate solution of the Navier–Stokes equations to be obtained; but it makes an intermediate join necessary, and the solution remains approximate in the limit of infinite Reynolds number, unlike boundary-layer solutions which become exact.

A number of extensions of the present work may be considered. The author has obtained (1959) outer solutions for which the pressure field was not necessarily conical, nor the radial velocity on the axis necessarily zero. For this more complicated problem it was convenient to introduce a stream function ψ, defined (in the present notation) by

$$U = 2\psi + \theta d\psi/d\theta, \quad W = \theta^2 d\psi/d\theta.$$

It turned out that $V^2 = K\psi$, with K = const., and the problem reduced to that of solving the ordinary non-linear equation

$$\theta^2 \frac{d^2\psi}{d\theta^2} + 3\theta \frac{d\psi}{d\theta} = -\frac{K}{2} + \frac{l}{\psi}, \tag{28}$$

where, in order that the velocity field be conical,

$$l = \frac{x}{2\rho}\left(\frac{\partial p}{\partial x}\right)_{\theta=\text{const.}} = \text{const.}$$

It was found, other conditions being equal, that a positive pressure gradient $\partial p/\partial x$ along θ_2 reduced the axial velocity within the core, increased the circumferential velocity, reduced the radial velocity, and increased the magnitude of the pressure difference $(p_2 - p)$. A negative pressure gradient had the reverse effect. The relaxation of the condition of zero radial velocity at the axis left the boundary condition W_2, which is a measure of the rate of flow into the core, free to be varied. It was found that small variations in W_2 produced comparatively large changes in the flow field within the core.

It should be mentioned that if the field for U and V is paraboloidal, depending on $\Theta = r/x^n$, n = const., instead of conical and dependent on θ, then (if one supposes that $x^{2n-2} = O(1)$ and $\Theta\, d\psi/d\Theta = O(\psi)$) an equation identical in form to (28) is obtained, with Θ replacing θ, and

$$L = \frac{x}{2n\rho}\left(\frac{\partial p}{\partial x}\right)_{\Theta=\text{const.}} = \text{const.}$$

replacing l. It is still true that $U = 2\psi + \Theta\, d\psi/d\Theta$ and $V^2 = K\psi$, but

$$W = nx^{n-1}\Theta^2 d\psi/d\Theta.$$

Therefore the solutions for U and V in a paraboloidal field, as functions of Θ, are identical to the solutions for U and V in a conical field, as functions of θ, for $L = l$.

Should practical reasons require the calculation of solutions for small perturbations of conical or paraboloidal field, or axial symmetry, this should be straightforward.

The present results also provide a basis for the investigation of 'vortex breakdown', an abrupt change in the flow from the pattern considered here, at some position downstream of the apex. This has been studied experimentally by Elle (1958), Peckham (1958), and Gray (unpublished), and theoretically by Squire (1960) and Jones (1960) who suggest plausible, but different, explanations for the phenomenon.

Finally, a first approximation to the temperature distribution in a real vortex core may be obtained by substituting the (incompressible) results for the velocity components into the energy equation, for example as Rott (1959) has done. This would constitute the first step in an iterative solution for a compressible vortex core.

REFERENCES

Cox, A. P. 1959 Measurements of the velocity at the vortex centre on an A.R.1 delta wing by means of smoke observations. *Aero. Res. Coun., Lond., Rep.* no. 21,116.

Earnshaw, P. B. 1961 An experimental investigation of the structure of a leading edge vortex. *Aero. Res. Coun., Lond., Rep.* no. 22,876.

Elle, B. J. 1958 An investigation at low speed of the flow near the apex of thin delta wings with sharp leading edges. *Aero. Res. Coun., Lond., Rep.* no. 19,780.

Hall, M. G. 1959 On the vortex associated with flow separation from a leading edge of a slender wing. *Aero. Res. Coun., Lond., Rep.* no. 21,117.

Hall, M. G. 1960 A theory for the core of a leading edge vortex. *Aero. Res. Coun., Lond., Rep.* no. 22,660.

Jeffreys, H. & Jeffreys, B. S. 1956 *Methods of Mathematical Physics*, 3rd ed. Cambridge University Press.

Jones, J. P. 1960 The breakdown of vortices in separated flow. *University of Southampton, U.S.A.A. Report*, no. 140.

Lambourne, N. C. & Bryer, D. W. 1959 Some measurements in the vortex flow generated by a sharp leading-edge having 65° sweep. *Aero. Res. Coun., Lond., Rep.* no. 21,073, *Curr. Pap.* no. 477.

Mangler, K. W. & Smith, J. H. B. 1959 A theory of the flow past a slender delta wing with leading edge separation. *Proc. Roy. Soc.* A, **251**, 200.

Newman, B. G. 1959 Flow in a viscous trailing vortex. *Aero. Quart.* **10**, 149.

Peckham, D. H. 1958 Low speed wind tunnel tests on a series of uncambered slender pointed wings with sharp edges. *Aero. Res. Coun., Lond., Rep.* no. 20,727.

Rott, N. 1959 On the viscous core of a line vortex. II. *Z. angew. Math. Phys.* **10**, 82.

Squire, H. B. 1960 Analysis of the 'vortex breakdown' phenomenon. Part 1. *Imperial College Aero. Dep., Rep.* no. 102.